CHAPTER

4

Optimization of in vitro conditions to study the arachidonic acid induction of 4R isoforms of the microtubule-associated protein tau

Yamini Mutreja, Truman C. Gamblin[1]

University of Kansas, Lawrence, KS, United States

[1]*Corresponding author: e-mail address: gamblin@ku.edu*

CHAPTER OUTLINE

Methods in Cell Biology, Volume 141, ISSN 0091-679X, http://dx.doi.org/10.1016/bs.mcb.2017.06.007

Abstract

The microtubule-associated protein tau exists in six different isoforms that accumulate as filamentous aggregates in a wide spectrum of neurodegenerative diseases classified as tauopathies. One potential source of heterogeneity between these diseases could arise from differential tau isoform aggregation. in vitro assays employing arachidonic acid as an inducer of aggregation have been pivotal in gaining an understanding of the longest four repeat tau isoform (2N4R). These approaches have been less successful for modeling the shorter 1N4R and 0N4R tau isoforms in vitro. Through a careful analysis of in vitro conditions for aggregation, we found that the differences in the acidity of tau isoform N-terminal projection domains determine whether tau filaments cluster into larger assemblies in solution. Beyond the potential biological implications of filament clustering, we provide optimized conditions for the arachidonic acid induction of shorter 4R tau isoforms aggregation in vitro that greatly reduce filament clustering and improved modeling results.

Abbreviations

4R	four-repeat
3R	three-repeat
AD	Alzheimer's disease
ARA	arachidonic acid
CBD	corticobasal degeneration
FTDP-17	frontotemporal dementia with parkinsonism linked to chromosome 17
LLS	laser light scattering
MTBR	microtubule-binding repeats
PSP	progressive supranuclear palsy
ThioS	thioflavin S
TEM	transmission electron microscopy

1 INTRODUCTION

The accumulation of filamentous aggregates of microtubule-associated protein tau is a pathological hallmark of several neurodegenerative disorders including Alzheimer's disease (AD) (Grundke-Iqbal et al., 1986; Wood, Mirra, Pollock, & Binder, 1986). In an adult human brain, six different isoforms of tau are generated by alternative splicing of exons 2, 3, and 10 from an mRNA encoded by a single gene (Goedert, Spillantini, Jakes, Rutherford, & Crowther, 1989; Goedert, Wischik, Crowther, Walker, & Klug, 1988). The C-terminal half of these proteins

contains imperfect repeat sequences of amino acids encoded by exons 9 through 12 (Himmler, Drechsel, Kirschner, & Martin, 1989). The pseudo-repeats contain motifs responsible for tau's interaction with microtubules called microtubule-binding repeats (MTBR) (Goode & Feinstein, 1994; Lee, Neve, & Kosik, 1989). The second repeat (MTBR2) is encoded by exon 10 and thus its presence or absence categorizes tau into either four-repeat (4R or 10^+) or three-repeat (3R or 10^-) isoforms, respectively. Alternative mRNA splicing of N-terminal exons 2 and 3 can change the number of acidic N-terminal inserts present within tau and give rise to isoforms with either two N-terminal inserts (2N isoforms), one N-terminal insert encoded by exon 2 (1N isoforms), or isoforms without either N-terminal insert (0N isoforms). Therefore, the six tau isoforms are designated 2N4R, 1N4R, 0N4R, 2N3R, 1N3R, and 0N3R (Goedert et al., 1989).

Expression of tau isoforms is both temporally and spatially regulated (Kosik, Orecchio, Bakalis, & Neve, 1989; Trabzuni et al., 2012). Isoforms are also known to exist in a specific ratio in the brain and disruption of this balance is associated with tauopathies (Chambers, Lee, Troncoso, Reich, & Muma, 1999; Conrad et al., 2007; Goedert et al., 1999; Hutton et al., 1998). The putative involvement of exon 10 in tau pathology has been extensively studied and its impact on tau pathology has been widely demonstrated (Schoch et al., 2016; Yoshida, 2006). A number of studies have pointed out the differences between 3R and 4R tau and how a disruption of the 3R to 4R tau balance could impact pathology: 3R tau differs from 4R tau in its stabilization of microtubules (Levy et al., 2005; Panda, Samuel, Massie, Feinstein, & Wilson, 2003), its aggregation (Adams, DeTure, McBride, Dickson, & Petrucelli, 2010; Combs, Voss, & Gamblin, 2011), and its seeding of the aggregation of monomeric tau (Dinkel, Siddiqua, Huynh, Shah, & Margittai, 2011). Disruption of the balance of the 3R to 4R tau isoform ratio has also been shown to affect anterograde vs retrograde transport of APP (Lacovich et al., 2017). However, the direct impact of exons 2 and 3 on tau pathology is less well understood. Recent evidence has established links between the inclusion and exclusion of the N-terminal inserts with increased pathology and disease (Baker et al., 1999; Caffrey, Joachim, & Wade-Martins, 2008; Ghanem et al., 2009), although the underlying mechanisms remain largely unclear. For example, the *MAPT* haplotype 2 resulting in higher levels of exon 3-containing transcripts of tau has been associated with reduced risk for tauopathies like progressive supranuclear palsy (PSP) and corticobasal degeneration (CBD) (Houlden et al., 2001). A weak association between tau haplotype and increased risk for AD has been identified (Allen et al., 2014), as well as reports of altered tau isoform expression in some cases of AD (Conrad et al., 2007). On a cellular level, the exogenous addition of Aβ42 peptide has been shown to favor the exclusion of exon 2 and 3 in tau transcripts in vitro (Lagunes, Herrera-Rivero, Hernandez-Aguilar, & Aranda-Abreu, 2014). Furthermore, altered expression of N-terminal variants of tau or unexpected patterns of their inclusion in aggregates have been identified in specific cases of frontotemporal dementia with parkinsonism linked to chromosome 17 (FTDP-17) and PSP (Lippa et al., 2000; Poorkaj et al., 2002; Rosso et al., 2002). It is likely that the N-terminal exons can play a significant

role in the underlying mechanisms leading to tau-induced neurodegeneration and therefore warrants more in-depth investigation.

In vitro model systems utilizing negatively charged species as the inducer of tau aggregation have been pivotal in gaining insights into the mechanisms resulting in tau aggregation and possible factors influencing its aggregation (Gamblin, King, Kuret, Berry, & Binder, 2000; Horowitz, LaPointe, Guillozet-Bongaarts, Berry, & Binder, 2006; von Bergen et al., 2006). One such model is the use of the polyunsaturated fatty acid arachidonic acid (ARA) to induce the aggregation of tau in vitro (Carlson et al., 2007). Fatty acid induction of tau aggregation may be of particular interest due to its potential biological role in the neurodegenerative process. For example, fatty acid metabolism is altered in pathology (Ong, Farooqui, & Farooqui, 2010; Snowden et al., 2017). A rise in lipid peroxidation products and increased concentration of free cytosolic polyunsaturated fatty acids has also been linked to several neurodegenerative disorders (Bradley-Whitman & Lovell, 2015; Sharon, Bar-Joseph, Mirick, Serhan, & Selkoe, 2003). Fatty acids are also the prime components of cellular membranes, and tau filaments have been observed to be either associated with or potentially growing out of membranes of neurons (Gray, Paula-Barbosa, & Roher, 1987). ARA-induced in vitro polymerization of tau is a widely established protocol and has successfully been used to model tau aggregation in vitro in a variety of studies, including the effects of phosphorylation, truncation, nitration, and FTDP-17-associated mutations in tau (Abraha et al., 2000; Combs & Gamblin, 2012; Reynolds, Berry, & Binder, 2005; Voss & Gamblin, 2009). However, the bulk of the ARA-induced aggregation studies of tau in vitro have focused on the 2N4R isoform. This could be due in part to the difficulties associated with in vitro ARA-induction of the 1N and 0N isoforms. For example, it has been reported that tau isoforms lacking exons 2 and 3 (the 0N isoforms of tau) fail to elongate into fibrils in the presence of ARA in vitro and only form short oligomeric aggregates of tau (King, Gamblin, Kuret, & Binder, 2000). To better understand the effect of disease-related changes on 0N and 1N isoforms of tau, there is a need for a more robust in vitro aggregation model system for these isoforms.

We hypothesized that the change in the isoelectric points of the N-terminal projection domain (residues 1–243) that would result from the inclusion or exclusion of exons 2 and 3 was responsible for the differences previously observed in the in vitro ARA induction of tau polymerization. We tested this hypothesis by altering the pH and ionic strength of both ARA-induced polymerization conditions and filament fixation conditions. We found that under normal in vitro polymerization conditions, the filaments formed by 1N4R and 0N4R isoforms have a tendency to aggregate into larger clusters of filaments. The degree of clustering was closely related to the overall charge of the N-terminal region. In conclusion, we show that by increasing the ionic strength of the in vitro ARA induction of tau aggregation, robust, and reliable amounts of aggregation of all three 4R isoforms can be obtained, opening new avenues for tau aggregation studies that have previously been hampered by these differences in isoform isoelectric points.

2 METHODS AND MATERIALS

2.1 PROTEIN EXPRESSION AND PURIFICATION

All wild-type 4R tau isoforms and corresponding pseudo-phosphorylated mutant proteins (7-phos) were expressed and purified as previously described (Combs et al., 2011; Rankin, Sun, & Gamblin, 2005). For the 7-phos proteins, mutations were introduced using the Quikchange site-directed mutagenesis kit (Agilent cat. 200,523). The 7-phos proteins contained the following mutations (numbered according to the 2N4R isoform) S199E, S202E, T205E, T231E, S235D, S396E, and S404E. DNA for all wild-type and mutant isoforms in the pT7C vector (with a 6 × histidine tag on the N-terminus) were transformed into BL-21 cells. Proteins were expressed and purified using nickel affinity chromatography followed by size exclusion chromatography as described previously. Final elution of protein was in a 10-mM HEPES buffer pH 7.64. Protein concentrations were determined using the Pierce™ BCA protein assay kit (Thermo Scientific cat. 23,225) following the manufacturer's protocol with BSA as a standard.

2.2 TAU POLYMERIZATION WITH ARA

Proteins at the concentration of 2 μM were incubated with ARA (Millipore cat. 181,198-100MG) to a final concentration of 75 μM in the polymerization buffer containing NaCl, 10 mM HEPES, pH 7.64, 0.1 mM EDTA, 5 mM DTT, and 3.75% ethanol (vehicle for ARA) for 24 h at 25°C. The standard final concentration of the NaCl in the tau polymerization reactions was 100 mM, but ranged from 100 to 250 mM dependent on the experiment (see Section 3). Control reactions (in the absence of ARA) were treated the same way as polymerization reactions except ARA was replaced with ethanol carrier for these reactions.

Tips:

- Handling of ARA: ARA is sensitive to light and oxidation. ARA from different vendors can be very different from one another. We have also found that ARA from the same vendor can vary from lot to lot. We routinely test ARA lots upon arrival using standard conditions for 2N4R tau aggregation to ensure that the batch of ARA is working similarly to previous batches. We are currently obtaining consistent batches of ARA from Millipore and Nu-Chek Prep. Once a vial obtained from a manufacturer is opened, the solution should be used within 1 month to avoid fluctuations in the amount of aggregation induced by ARA. To prepare ARA stocks for storage, 100% ethanol was added directly to the vial obtained from the manufacturer to obtain a 25-mg per 1 mL stock. It is helpful to "wet" the pipette tip by pipetting the ethanol up and down approximately six times to ensure delivery of the appropriate amount of ethanol. The ARA/ethanol dilutions are mixed gently by shaking to avoid excess introduction of atmospheric oxygen into the stock solutions. The 25 mg/mL ARA solution in ethanol was

transferred to amber colored 0.5 mL microcentrifuge tubes in 20–25 μL aliquots and stored at −80°C until needed. Once ready to set up tau polymerization reactions, the ARA storage stock was used to make a 2-mM working stock using ethanol. The working stock was kept on ice and used within 2–3 h to set up polymerization reactions. Each aliquot was used for one experiment and then discarded.

- Setting up tau polymerization reactions: The order of addition and ensuring sufficient mixing after addition of each component are important determinants in obtaining consistent levels of tau aggregation. Various components were added to ultrapure water (Cayman Chemicals cat. 400,000) in the following order: DTT, NaCl, HEPES, EDTA, and protein. Solutions were mixed by pipetting up and down 10 times after addition of each component. ARA was added to a final concentration of 75 μM (from the 2 mM working stock) resulting in a final ethanol concentration of 3.75%. It is important to "wet" the pipette tip by pipetting up and down approximately six times before transferring the ARA to ensure consistent delivery of the desired volume. A uniform mixing after ARA addition was obtained by gently tapping the side of microcentrifuge tubes before incubation at 25°C. We generally use clear microcentrifuge tubes in order to watch the mixing of the components as they are added to help ensure thorough mixing.

2.3 FIXATION OF TAU FILAMENTS AND ELECTRON MICROSCOPY

2.3.1 Fixation

For experiments to determine the effect of pH (Figs. 2 and 4), polymerization reactions performed at the standard conditions of salt (100 mM NaCl) and pH (7.64) were diluted 1:10 in a buffer of selected pH (dependent on the experiment) along with the fixative glutaraldehyde (Electron Microscopy Sciences cat. 16,120) at a final concentration of 2%. Buffers used for dilution at specific pH were CAPS (pH 10), CHES (pH 8.7), HEPES (pH 7.64), MOPS (pH 6.8), MES (pH 6.1 or 6), and acetate (pH 5). All buffers were used at a 10-mM strength with 0.1 mM EDTA and 100 mM NaCl (same as polymerization conditions).

For experiments looking at the effect of pH at higher ionic strength (Fig. 3), polymerization reactions set up at the standard conditions of salt (100 mM NaCl) and pH (7.64) were diluted 1:10 in a fixation buffer that contained 200 mM NaCl instead of 100 mM at the pH values indicated in Fig. 3.

For rest of the experiments (Figs. 1, 5, and 7), polymerization reactions were set up and diluted 1:10 for fixation in 10 mM HEPES buffer, pH 7.64 with 0.1 mM EDTA. The concentration of NaCl in the fixation buffer was identical to the buffer utilized for polymerization.

After a 5-min fixation at chosen conditions, samples were deposited on a formvar-coated copper grid (Electron Microscopy Sciences cat. FCF-300CU) and stained with 2% uranyl acetate according to the previously published protocol (Combs et al., 2011). Briefly, 10 μL of diluted and fixed polymerization reactions are pipetted onto a piece of parafilm. EM grids are placed on top of the drop where

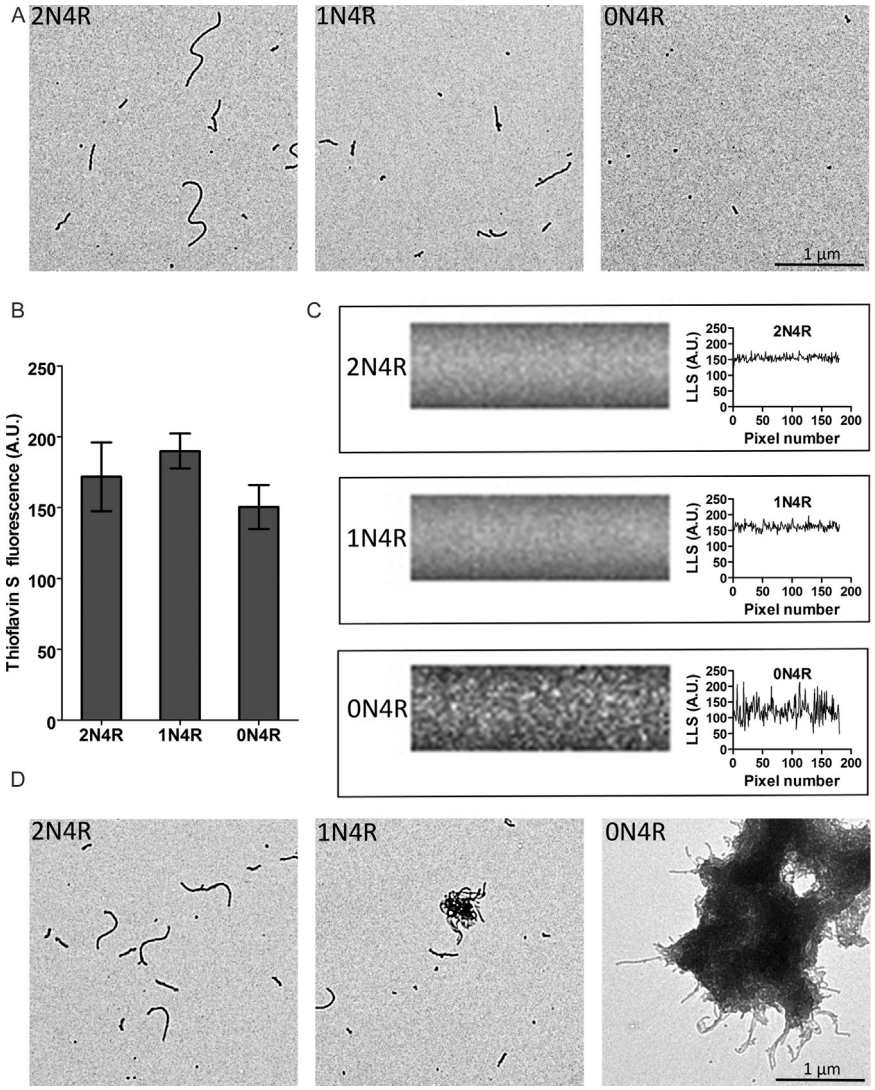

FIG. 1

Discrepancies in ARA-induced polymerization of 4R tau N-terminal variants. 2 μM protein was polymerized using 75 μM ARA overnight at 25°C under standard salt and pH conditions. (A) Electron micrographs of polymerized proteins obtained via a random selection criterion. (B) Extent of polymerization measured using ThioS fluorescence. Each bar represents data from three independent experiments ±SD. (C) Right-angle laser light scattering images (*left*) and the corresponding intensity of pixels across the width (*right*) for various 4R tau filaments. (D) Electron micrographs obtained via searching the grids to obtain images of filament clusters, which are not evenly distributed. Scale bar is 1 μm and is applicable to each image.

they float for 1 min. The grid is then blotted on filter paper, placed on a drop of water, blotted with filter paper, placed on a drop of 2% uranyl acetate, and blotted dry. All drops are 10 μL pipetted onto parafilm. The grid is then placed on another drop of 2% uranyl acetate and floated for 1 min, and blotted dry for a final time. To ensure consistency between grids, fixation times are not allowed to exceed 15 min. Care should be taken handling glutaraldehyde and uranyl acetate.

2.3.2 Electron microscopy data collection

FEI TECNAI F20 XT field emission electron microscope (Hillsboro, OR) was used to examine the grids at a magnification of 3600×. Images were captured with the Gatan Digital Micrograph imaging system. Two different methods were employed to collect images: (i) a *random* selection method was utilized to minimize user bias. Under this method, five different areas of a grid were selected at random and images were captured. (ii) A *search* method was utilized to locate the less frequently encountered clusters of filaments. Here, the grid was searched until filament clusters were found and then images were captured. In general, five images are collected per grid.

2.4 CHARGE PREDICTIONS

PROTEIN CALCULATOR v3.4 by Scripps Research Institute (http://protcalc.sourceforge.net/) was used to calculate the charges of N-terminal projection domain of 4R tau isoforms at several pH values.

2.5 THIOFLAVIN S FLUORESCENCE

Thioflavin S (ThioS) (Sigma cat. T1892) was dissolved in MilliQ water at a concentration of 0.224 mg/mL followed by filtration through a 0.22-μm filter. The ThioS solution was protected from light, prepared, and used the same day. 150 μL of polymerization reactions were transferred to a 96-well, flat bottom, white plate. 6 μL of ThioS solution was added to each well. The plate was shaken for 30 s followed by an incubation in the dark for 20 min. An excitation wavelength of 440 nm and an emission wavelength of 520 nm was used to record the shift in fluorescence resulting from ThioS binding to tau aggregates (King, Ahuja, Binder, & Kuret, 1999) using a Cary Eclipse fluorescence spectrophotometer (Varian Analytical Instruments, Walnut Creek, CA). Control reactions were used to determine the background fluorescence readings, and these values were subtracted from experimental wells.

2.6 RIGHT ANGLE LASER LIGHT SCATTERING

Polymerized protein solutions were transferred to 5 mm × 5 mm optical glass fluorometer cuvettes (Starna Cells, Atascadero, CA) and illuminated with a 12-mW solid state laser with a wavelength of 532 nm and operating at 7.6 mW (B&W Tek, Inc., Newark, DE). An image of the amount of light scattered was captured at the angle perpendicular to the path of the laser using a SONY XC-ST270 digital camera at an

aperture setting of 5.6–8. Precise conditions should be optimized for each specific laser and camera setup. The images were analyzed using the histogram function of Adobe Photoshop CS5 Version 12.0 ×32 to obtain a mean intensity indicative of the amount of light scattered. A fixed area (150 px × 15 px) was selected from each image, and the mean density was recorded to represent the amount of light scattered for each condition. For calculating the pixel intensity across an image of scattered light, the plot profile function of ImageJ was used for a 180 pixels wide line.

2.7 KINETICS OF AGGREGATION

Although data are not presented in this report, these methods can be used to follow the kinetics of tau polymerization. For right angle laser light scattering, reactions are prepared in a microcentrifuge tube and transferred to 5 mm × 5 mm optical glass fluorometer cuvettes before the addition of ARA. The amount of background scattering without ARA is measured and is used for background subtraction. ARA is added, gently mixed, and the amount of scattering is immediately captured (time zero). Images of scattered light are generally taken at 5, 10, 15, 20, 25, and 30 min. Images are then taken at 45 and 60 min, followed by captures at 90, 120, 180, 240, 300, and 360 min. ARA-induced polymerization reactions generally have reached an apparent steady state after 6 h of incubation. Similarly, the kinetics of polymerization reactions can be followed using electron microscopy, although this method is much more involved and time consuming. For this approach, reactions are performed in microcentrifuge tubes and then samples are taken at various time points, fixed, and EM grids are prepared for viewing and quantitation. We often reduce the number of time points taken using this approach. In general, we do not use ThioS for measuring kinetics of reactions because we have found that the addition of ThioS at the beginning of an ARA-induction of tau polymerization enhances the rate and amount of aggregation.

3 RESULTS

3.1 PROBLEMS ASSOCIATED WITH ARA-INDUCED IN VITRO AGGREGATION OF SHORTER HUMAN TAU ISOFORMS

ARA polymerization has been utilized in a number of studies targeted to investigate several aspects of tau aggregation in vitro (Abraha et al., 2000; Combs & Gamblin, 2012; Reynolds et al., 2005; Voss & Gamblin, 2009). Using this technique, recombinantly expressed human tau isoforms are incubated in the presence of ARA in buffer containing 100 mM NaCl, 10 mM HEPES, pH 7.64, 5 mM DTT, and 0.1 mM EDTA. Under these conditions, 2N4R and 1N4R isoforms polymerize to form filamentous aggregates of tau reminiscent of straight fibrils associated with AD and other tauopathies (Fig. 1A). However, as previously reported, the 0N4R isoform fails to form straight filaments that are easily detectable by electron microscopy

(Fig. 1A). This result is confounded by the observation that ARA-induced 0N4R isoform polymerization reactions do have ThioS reactivity to an extent comparable with 2N4R and 1N4R isoforms (Fig. 1B). There also seems to be an isoform-dependent difference in the appearance of laser light scattered by the filaments. The light scattered by the 0N4R isoform often has a speckled appearance, with density missing from certain regions and oversaturated foci of scattered light in other areas, in contrast to the light scattered by the 2N4R and 1N4R isoforms which has a smoother, more uniform appearance (Fig. 1C).

The observed discrepancies between ThioS fluorescence and TEM data combined with the anomalous speckled appearance of the light scattered by the 0N4R isoform compared to the longer N-terminus variants, raised the possibility that the 0N4R tau filaments were conglomerating in solution. To investigate this possibility, we performed a thorough search of the microscopy grids for 0N4R isoform polymerization reactions rather than the standard operating procedure of randomly selecting areas of the grid for viewing to reduce observer bias in field selection. Large, amorphous structures with heavy stain accumulations, and with what appeared to be filaments protruding from their edges were observed in 0N4R polymerization reactions using the search method (Fig. 1D). Clusters of tau filaments were also occasionally detected with thorough searching of EM grids for 1N4R polymerization reactions (Fig. 1D), but these clusters were smaller and accumulated less uranyl acetate stain than those observed with 0N4R isoforms. Clusters of 2N4R isoform filaments could not be found under these experimental conditions even with extensive searching (Fig. 1D). It is clear from this data that the filaments formed from N-terminal variants of 4R isoforms have distinct solution characteristics from one another under these conditions.

3.2 DIFFERENTIAL ELECTROSTATICS OF THE TAU N-TERMINAL PROJECTION DOMAIN AND ITS ROLE IN FILAMENT CLUSTERING

One fundamental difference between these isoforms is in their primary structure. Exons 2 and 3 each contain 29 amino acids and both regions are acidic in nature (below):

```
          -        --  --   -  - +     -    Net charge
Exon 2 ESPLQTPTEDGSEEPGSETSDAKSTPTAE      -7
          -       --    +        -  -
Exon 3 DVTAPLVDEGAPGKQAAAQPHTEIPEGTT      -4
```

At the standard working pH of 7.64, the N-terminal projection domain of the 2N4R (exons 2 and 3), 1N4R (exon 2 only), and 0N4R (neither exon) isoforms are predicted to have an overall charge of −5.6, −1.7, and +5.3, respectively (Table 1). The N-terminal projection domain remains largely disordered and protrudes from the filament core formed by the MTBR region of tau (Novak, Jakes, Edwards, Milstein, & Wischik, 1991; von Bergen et al., 2006; Wegmann, Medalsy, Mandelkow, & Muller, 2013; Wischik et al., 1988). We therefore hypothesized

Table 1 Theoretical Net Charge Carried by the Projection Domain (Amino Acids 1–243, Along With the Histidine Purification Tag) of Various 4R Tau N-Terminal Variants Over a pH Range

pH	2N4R	1N4R	0N4R
4.00	+31.5	+31.0	+32.2
4.50	+21.3	+22.1	+25.6
5.00	+12.1	+14.1	+19.5
5.50	+6.7	+9.4	+15.9
6.00	**+3.3**	**+6.4**	**+13.2**
6.50	−0.2	+3.2	+10.2
7.00	−3.4	+0.4	+7.4
7.50	−5.3	−1.4	+5.6
7.64	**−5.6**	**−1.7**	**+5.3**
8.00	−6.4	−2.4	+4.6
8.50	−7.3	−3.3	+3.7
9.00	−8.9	−4.8	+2.3
9.50	−12.3	−8.0	−0.8
10.00	**−18.1**	**−13.6**	**−6.1**

Experimentally studied pH values are indicated in bold. *The cells colored in* dark gray *represent pH values at which the projection domain of each isoform is predicted to carry an overall positive charge.* Light gray *cells represent the pH values at which the projection domain of each isoform is predicted to carry an overall negative charge.*

that the clustering of 1N and 0N filaments is an outcome of the lower acidity and the overall charge of the N-terminal projection domain extending from the filament core.

To test whether the decreasing acidity of the N-terminal projection domain leads to filament clustering through electrostatic interactions, we sought to counter this effect by either altering the pH or increasing the ionic strength of the solution-containing tau filaments. Unlike what is predicted for the standard pH of 7.64, all three isoforms would have positively charged projection domains at a pH of 6.0, and all three isoforms would have negatively charged projection domains at a pH of 10.0 (Table 1).

We first investigated the effects of pH on tau filament clustering by varying pH at the time of fixation. Polymerization reactions were performed as previously described using standard conditions of 2 μM protein and 75 μM ARA in 10 mM HEPES buffer, pH 7.64, and 100 mM NaCl. After 16 h of incubation, samples were prepared for electron microscopy. Samples were fixed with 2% glutaraldehyde in buffers with different pH values chosen to alter the overall charge of the N-terminal projection domain: all positively charged (pH 6); standard conditions with different charges (pH 7.64); and all negatively charged (pH 10) (see Table 1). As predicted, buffer conditions for positively charged N-terminal projection domains (pH 6) result in

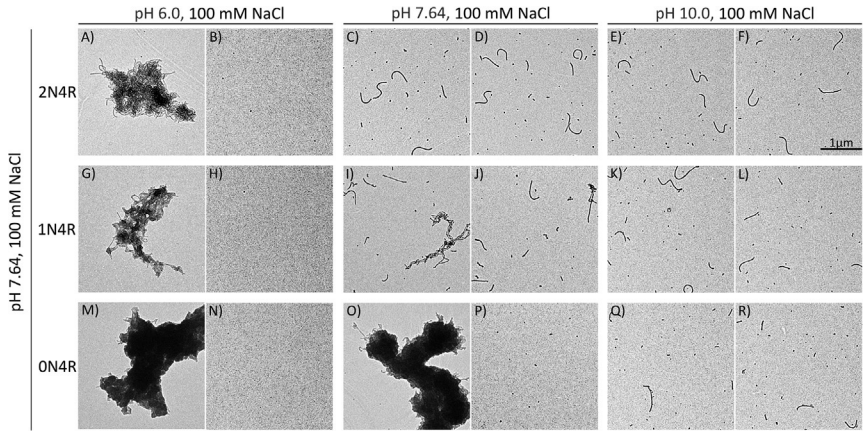

FIG. 2

Effect of pH on filament clustering. Electron micrographs of 4R proteins polymerized using 2 μM protein and 75 μM ARA under the standard conditions of 100 mM NaCl at pH 7.64 (vertical axis), with filament fixaton conditions represented on the horizontal axis. Two images for each working condition are presented. Images on the *right side* for each panel (Images B, D, F, H, J, L, N, P, and R) were obtained using a random selection to minimize bias, and images on the *left side* for each panel (Images A, C, E, G, I, K, M, O, and Q) were obtained after extensive searching to locate clusters of filaments. Scale bar in image (F) represents 1 μm and is applicable to all images.

filament clusters for all three 4R tau isoforms that could be located on EM grids with searching (Fig. 2A, G, and M). Under these conditions, most EM fields of view selected at random had few filaments with only small particles of tau visible (Fig. 2B, H, and N). Fixation buffer conditions for negatively charged N-terminal projection domains (pH 10) resulted in even distributions of single strands of tau filaments on the electron microscopy grid for all three 4R isoforms, even with extensive searching (Fig. 2E, F, K, L, Q, and R). The 0N4R isoform, previously thought to only make small oligomeric aggregates with ARA (King et al., 2000), also showed filamentous tau aggregates when fixed at pH 10 (Fig. 2Q and R), suggesting the possibility that the increase in pH causes clusters of filaments to dissociate during the fixation process.

The modulation of filament clustering by changes in pH is consistent with the hypothesis that this phenomenon is mediated through electrostatic interactions. To further test this model, we sought to determine whether filament clustering observed under standard polymerization conditions could be disrupted with increased ionic strength. Tau aggregation reactions were again performed under standard conditions of pH 7.64 and 100 mM NaCl. Tau filaments were subsequently diluted in buffers containing higher amount of salt (200 mM) before glutaraldehyde fixation in buffers with the same low (6), standard (7.64), and high (10) pH values examined

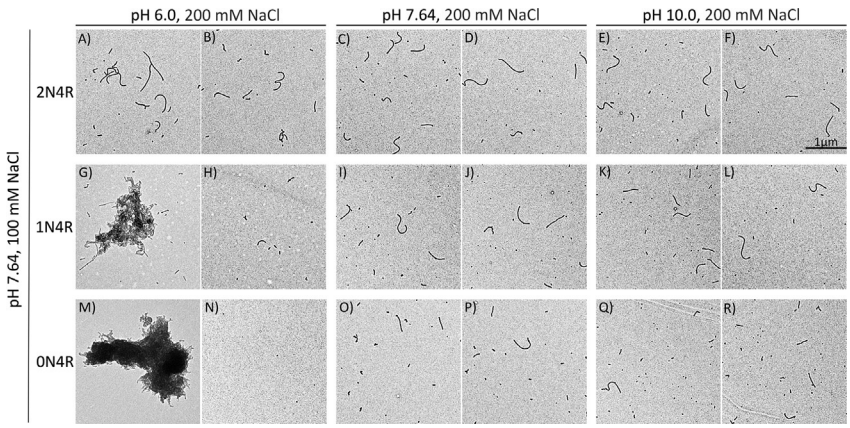

FIG. 3

Countering the effect of pH by increasing ionic strength. Electron micrographs of 4R proteins polymerized using 2 μM protein and 75 μM ARA under the standard conditions of 100 mM NaCl at pH 7.64 (vertical axis), with filament fixation conditions represented on the horizontal axis. Two images for each working condition are presented. Images on the *right side* for each panel (Images B, D, F, H, J, L, N, P, and R) were obtained using a random selection to minimize bias, and images on the *left side* for each panel (Images A, C, E, G, I, K, M, O, and Q) were obtained after extensive searching to locate clusters of filaments. Scale bar in image (F) represents 1 μm and is applicable to all images.

earlier. Increased ionic strength of fixation buffers drastically decreased filament clustering (Fig. 3). For example, the clustering of 0N4R filaments was essentially eliminated when the filaments were fixed at pH 7.64 and 200 mM NaCl (compare Figs. 2O–P and 3O–P). The increased ionic strength also drastically reduced the amount of 2N4R isoform filament clustering observed at pH 6 (compare Figs. 2A and B and 3A and B). Therefore, increased ionic strength reduced the degree of filament clustering in a manner that correlates with the degree of negative charges in the N-terminal projection domains.

3.3 CHANGE IN THE ACIDITY OF THE PROJECTION DOMAIN OF TAU THROUGH PSEUDO-PHOSPHORYLATION IMPACTS FILAMENT CLUSTERING

The previous results indicate that the clustering of filaments is due to electrostatic interactions involving the N-terminal projection domain, and more negatively charged amino acids in this region reduce clustering of tau filaments. We tested this directly by comparing nonmodified protein with "pseudo-phosphorylated" versions. Pseudo-phosphorylation involves the mutation of serines and threonines to aspartic or glutamic acids. We used proteins called 7-phos because they have

Table 2 Theoretical Net Charge Carried by the Projection Domain (Amino Acids 1–243, Along With the Histidine Purification Tag) of Various 4R Tau Wild-Type and Pseudo-Phosphorylation (7-Phos) N-Terminal Variants at Three Distinct pH Values (High, Intermediate, Low) Chosen on an Isoform-Specific Basis

Net Charge (Projection Domain)			
Protein	**pH**	**Wild-Type**	**7-Phos**
2N4R	High (7.64)	−5.6	−10.6
	Intermediate (6.1)	+2.6	−2.3
	Low (5)	+12.1	+8.1
1N4R	High (10)	−13.6	−18.6
	Intermediate (6.8)	+1.4	−3.6
	Low (6)	+6.4	+1.5
0N4R	High (10)	−6.1	−11.1
	Intermediate (8.7)	+3.3	−1.7
	Low (6)	+13.2	+8.3

The cells colored in dark gray *represent pH values at which the projection domain of each isoform is predicted to carry an overall positive charge.* Light gray *cells represent the pH values at which the projection domain of each isoform is predicted to carry an overall negative charge.*

seven different phosphorylation-mimicking mutations. Five of these residues (S199E, S202E, T205E, T231E, and S235D) are located in the N-terminal projection domain and the other two (S396E and S404E) are in the C-terminal region.

Due to the presence of additional acidic residues, the pH at which the projection domains of pseudo-phosphorylated proteins would become positively charged and thus potentially result in filament clustering are expected to be lower than their wild-type counterparts (Table 2). We compared all three 4R isoforms wild-type proteins with their pseudo-phosphorylated forms using ARA and standard buffer conditions of 100 mM NaCl and pH 7.64. The fixation conditions were chosen on an isoform-specific basis for high pH (both negatively charged), intermediate pH (different charges for N-terminal projection domains), and low pH (both positively charged) (Table 2).

The filaments formed by all three pseudo-phosphorylated 4R isoforms required a lower pH than their corresponding wild-type proteins for clustering (Fig. 4A–C). For example, an even distribution of filaments was observed for the 7-phos 1N4R protein at pH 6.8 (negatively charged), while the wild-type 1N4R filaments (positively charge at this pH) were completely clustered (Fig. 4B). An even distribution of filaments was observed at pH 10 (both negatively charged) for both these proteins, while filaments of both wild-type and pseudo-phosphorylated proteins clustered at pH 6 (positively charged). These results indicate that the pseudo-phosphorylation did not change the overall pattern of response of filament–filament interaction to changing pH, but rather changed the pH at which filaments clustered. Conditions that

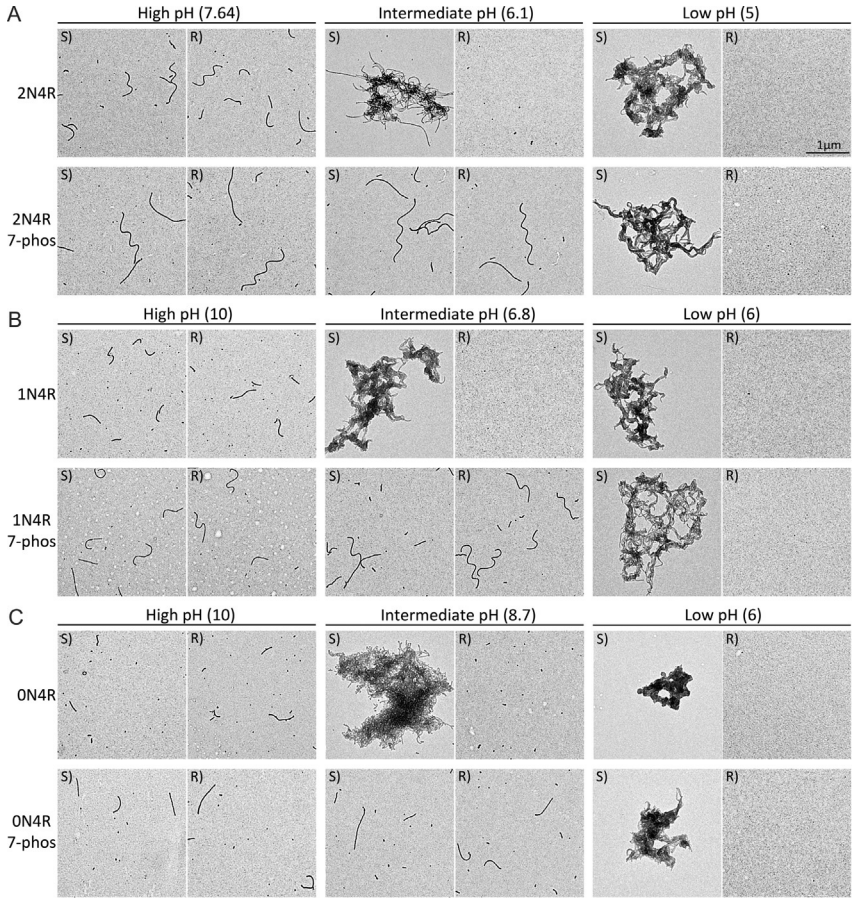

FIG. 4

Enhanced acidity of projection domain by pseudo-phosphorylation reduces sensitivity to clustering. Electron micrographs of (A) 2N4R, (B) 1N4R, and (C) 0N4R proteins (wild-type and 7-phos variants) polymerized using 2 μM protein and 75 μM ARA under the standard conditions of 100 mM NaCl at pH 7.64. Fixation buffer contained 100 mM NaCl at all the indicated pH values. Two images for each working condition are presented. Images on the *right side* of each panel (designated as R) were obtained using a random selection to minimize bias, and images on the *left side* of each panel (designated as S) were obtained after extensive searching to locate clusters of filaments. Scale bar in upper right panel represents 1 μm and is applicable to all images.

result in a positively charged N-terminal projection domain resulted in filament clustering, and conditions that result in a negatively charged N-terminal projection domain reduced filament clustering as demonstrated by even distributions of filaments on the EM grid.

3.4 EFFECT OF POLYMERIZATION BUFFER SALT CONCENTRATION ON TOTAL AMOUNT OF AGGREGATION OF TAU ISOFORMS

Because increasing the ionic strength of the fixation buffer or increasing its pH to 10 prevented the clustering of 1N4R and 0N4R filaments, we sought to determine whether employing these conditions during the polymerization reaction itself would have similar results.

Increasing the pH for our tau polymerization reaction to pH 10 inhibited tau aggregation completely (data not shown). There could be several explanations for this outcome. One reason could be that rise in pH could change the micellar state of ARA which in turn can alter its ability to cause tau aggregation. Another possible reason could be that a rise in pH may alter the conformation of tau and render it incapable of aggregation.

We sought to determine whether increasing the ionic strength during polymerization would eliminate the clustering without compromising the total amount of aggregation of 4R tau isoforms. ARA-induced polymerization reactions were performed using pH 7.64 and 200 mM NaCl instead of 100 mM NaCl. Under these conditions, the filaments for all three isoforms were evenly distributed on the grid when fields were selected randomly. Clusters of filaments were not detected for any of the three isoforms even with extensive searching (Fig. 5A). Furthermore, laser light scattered by the filaments assembled at 200 mM NaCl for 0N4R tau also had a smooth appearance (Fig. 5B) unlike the speckled appearance observed at 100 mM NaCl (compare Fig. 1C with Fig. 5B).

To compare the overall levels of tau polymerization with increasing ionic strength, 2 μM protein was incubated with 75 μM ARA for 24 h at pH 7.64 and NaCl ranging from 100 to 250 mM. At the end of the incubation period, the extent of polymerization was measured by two different techniques, a laser light scattering assay (Fig. 6A) and a ThioS fluorescence assay (Fig. 6B). None of these salt concentrations had any significant impact on the total amount of polymerization of any of the 4R isoforms of tau to a level detectable within the error of the techniques employed.

Overall, increasing the ionic strength of the polymerization buffer or fixation buffer improved the utility of electron microscopy data for shorter tau isoforms, possibly by overcoming the electrostatic interactions causing filament clustering (Figs. 2 and 5) without inhibiting the process of tau aggregation to any significant extent (Fig. 6).

3.5 UTILITY OF NEW AGGREGATION CONDITIONS FOR IN VITRO AGGREGATION STUDIES OF MIXED TAU ISOFORMS

Efforts to coaggregate different 4R tau isoforms have proven to be difficult. Using the physiological ratio of 2N:1N:0N 4R isoforms of 9:54:37 (Goedert & Jakes, 1990; Hong et al., 1998), a final, total protein concentration of 2 μM was induced with

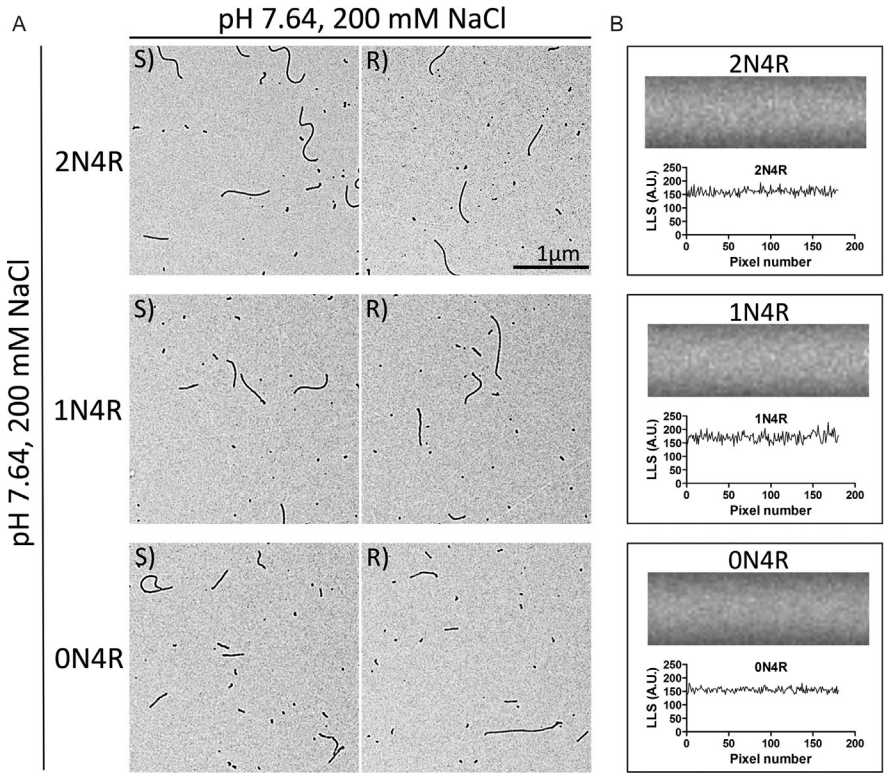

FIG. 5

Polymerization at 200 mM NaCl eliminates clustering of filaments for all 4R tau isoforms and anomalous light scattering for 0N4R isoform. 4R proteins polymerized using 2 μM protein and 75 μM ARA. (A) Electron micrographs of tau isoforms polymerized and fixed using a buffer containing 200 mM NaCl at pH 7.64. Two images for each working condition are presented. Images on the *right side* of each panel (designated as R) were obtained using a random selection to minimize bias, and images on the *left side* of each panel (designated as S) were obtained after extensive searching to locate clusters of filaments. (B) Right-angle laser light scattering images (*top*) and the corresponding intensity of pixels across the width (*bottom*) for polymerized 4R tau isoforms.

75 μM ARA at 100 mM NaCl (pH 7.64). These conditions resulted in clusters of aggregates that can be encountered frequently on the electron microscopy grid (Fig. 7A). Increasing the ionic strength of polymerization reactions to 200 mM NaCl eliminates the clustering of tau filaments completely (Fig. 7A) without impacting the overall levels of polymerization, when measured using laser light scattering (Fig. 7B) or ThioS fluorescence (Fig. 7C).

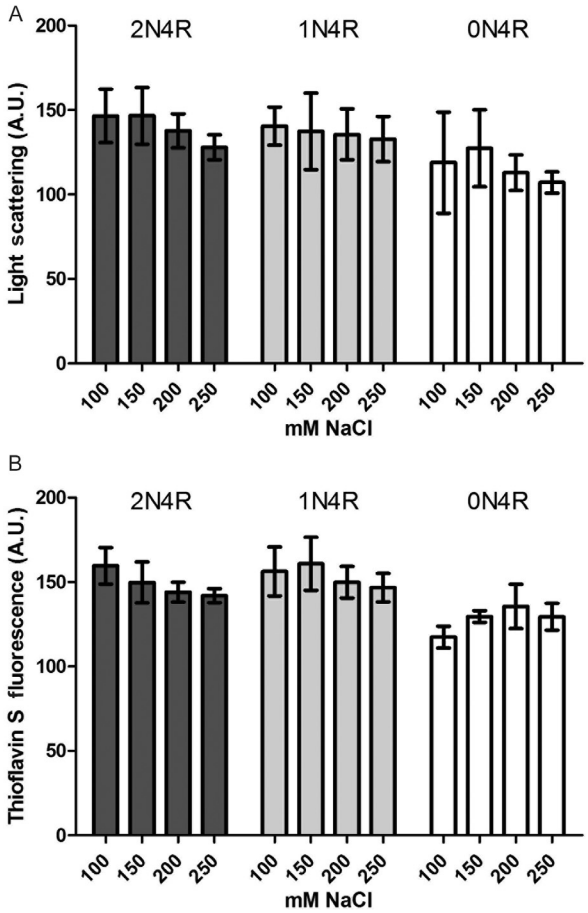

FIG. 6

Polymerization of 4R tau proteins at varying amounts of salt. 2 μM 4R proteins polymerized using 75 μM ARA in HEPES buffer pH 7.64 containing salt concentrations ranging from 100 to 250 mM overnight at 25°C. The final extent of polymerization was measured by (A) ThioS fluorescence and (B) right-angle laser light scattering (LLS). Each bar represents data from three independent experiments ±SD. One-way ANOVA analysis with Turkey's multiple comparison test was used to determine the statistical significance of data obtained for each isoform at different salt concentrations for each of the techniques employed, LLS and ThioS fluorescence.

It is not entirely known if various N-terminus variants of 4R tau isoforms can copolymerize or seed the aggregation of other tau N-terminal variants. Unreliable polymerization of 0N4R tau isoform has previously hampered such studies. Here, we present a model of copolymerization of N-terminus variants of tau that can be employed to answer such questions in future (Fig. 7).

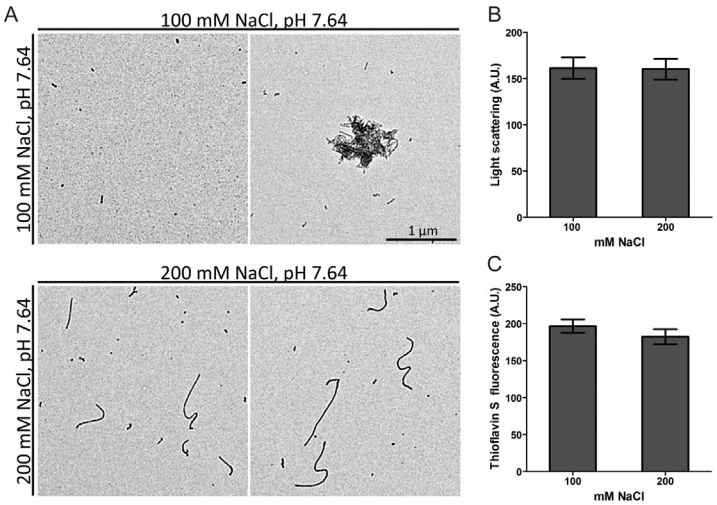

FIG. 7

Aggregation of mixture of 4R tau isoforms. 4R proteins at a molar ratio of 2N:1N:0N, 9:54:37 polymerized using 2 μM total protein and 75 μM ARA at the salt and pH conditions indicated on the vertical axis, with filament fixaton conditions represented on the horizontal axis. (A) Two images are presented to represent the uneven distribution of tau filaments resulting from clustering of tau filaments at 100 mM NaCl; extent of polymerization measured using (B) laser light scattering and (C) ThioS fluorescence. Each bar represents data from three independent experiments ±SD. Student's unpaired two-tailed *t*-test was performed to estimate the level of significance.

4 DISCUSSION AND CONCLUSIONS

Aggregation of tau is a central event in the course of numerous neurodegenerative disorders (Sergeant, Delacourte, & Buee, 2005). An in vitro model employing ARA as an inducer of tau aggregation has helped gain insight into the pathological mechanisms and factors influencing this event (Combs & Gamblin, 2012; Gamblin et al., 2000). While this is true for the 2N4R isoform of tau, a reliable interpretation of data for the 1N4R and 0N4R isoforms of tau has been a challenging task (Fig. 1) (King et al., 2000). In this study, we have identified filament clustering of shorter isoforms of tau as a reason behind some of these complexities. Our data suggest that the electrostatic interactions involving the unstructured N-terminal projection domain of tau protruding from the filament core influences this clustering behavior.

Specifically, we observed an inverse relationship between the acidity of tau N-terminal projection domain and the propensity of tau filaments to cluster. First, exclusion of the acidic N-terminal inserts rendered the filaments formed by 0N and 1N isoforms of tau more sensitive to fluctuations in pH and salt and caused them

to form clusters of filaments. Modulating the pH, and thus altering the overall charge carried by the N-terminal projection domain, indicated that a positively charged N-terminal projection domain results in filament clustering while this clustering behavior can be overcome by making the N-terminal projection domain negatively charged (Table 1 and Fig. 2). Second, this hypothesis could be corroborated by utilizing mutations that raise the acidity of N-terminal projection domain (pseudo-phosphorylation). Pseudo-phosphorylated 4R tau isoforms require a lower pH to form clusters of filaments (Fig. 4).

Interestingly, Wegmann et al. observed that the adhesive properties of the "fuzzy coat," formed by the unstructured regions of tau protruding from the filament core, change with pH and ionic strength of the environment surrounding tau filaments (Wegmann et al., 2013). Moreover, they observed that lowering the pH and thus making the fuzzy-coat overall positively charged enhanced adhesion to negatively charged particles. The reason behind a positively N-terminal projection domain leading to a tau filament clustering observed in our study is not yet clear but negatively charged species such as the fatty acid ARA (also present in the solution) could play a role in facilitating the interactions between tau filaments, although more work would be needed to decipher their exact role. Nonetheless, this study sheds light into some of the processes that could affect the association of tau filaments with each other which may be of biological relevance.

Association of filaments with each other is thought to be a fundamental process for formation of macroscopic pathological tau aggregates, such as neurofibrillary tangles. Here we observed that the unstructured N-terminal projection domain could be a driving factor behind such "tangle-like" interactions. It can also be speculated that the electrolytic perturbances associated with aging and pathology (Mattson, Mark, Furukawa, & Bruce, 1997) could be played a role in the process. Moreover, it is important to note that such changes would have a differential effect on the N-terminal variants of tau. In addition to the effect of electrolytes and ions, we observed a phenomenon of tau filament clustering at low pH values. It is tempting to speculate that the low lysosomal pH could be implicated in affecting the properties of tau filaments and potentially altering tau filament–filament association.

Biological consequences of this charge driven association of tau filaments will need to be tested in future studies; nonetheless, the current study has immediate consequences in modeling of ARA-induced aggregation of tau isoforms in vitro. We were able to overcome the clustering behavior of tau filaments by elevating the ionic strength in our tau polymerization protocol (Fig. 5). This update in the current protocol of ARA-induced tau aggregation of isoforms could help devise future studies of various aspects of tau polymerization that may have isoform-specific effects, like tau mutations, posttranslational modifications, tau seeding, and looking at the effect of previously identified tau aggregation inhibitors (Paranjape et al., 2015) on various tau isoforms.

ACKNOWLEDGMENTS

We thank Adam Miltner for assistance with protein purification. We also thank Dr. Mythili Yenjerla for advice and helpful suggestions and for her work on a related project that helped advance this study.

Funding: This work is supported by NIH R01 NS083391 (T.C.G.) and a Mabel A. Woodyard Fellowship from the Institute for Neurological Discoveries at the University of Kansas Medical Center (Y.M.).

REFERENCES

Abraha, A., Ghoshal, N., Gamblin, T. C., Cryns, V., Berry, R. W., Kuret, J., et al. (2000). C-terminal inhibition of tau assembly in vitro and in Alzheimer's disease. *Journal of Cell Science*, *113*(Pt. 21), 3737–3745.

Adams, S. J., DeTure, M. A., McBride, M., Dickson, D. W., & Petrucelli, L. (2010). Three repeat isoforms of tau inhibit assembly of four repeat tau filaments. *PloS One*, *5*(5), e10810.

Allen, M., Kachadoorian, M., Quicksall, Z., Zou, F., Chai, H. S., Younkin, C., et al. (2014). Association of MAPT haplotypes with Alzheimer's disease risk and MAPT brain gene expression levels. *Alzheimer's Research & Therapy*, *6*(4), 39.

Baker, M., Litvan, I., Houlden, H., Adamson, J., Dickson, D., Perez-Tur, J., et al. (1999). Association of an extended haplotype in the tau gene with progressive supranuclear palsy. *Human Molecular Genetics*, *8*(4), 711–715.

Bradley-Whitman, M. A., & Lovell, M. A. (2015). Biomarkers of lipid peroxidation in Alzheimer disease (AD): An update. *Archives of Toxicology*, *89*(7), 1035–1044.

Caffrey, T. M., Joachim, C., & Wade-Martins, R. (2008). Haplotype-specific expression of the N-terminal exons 2 and 3 at the human MAPT locus. *Neurobiology of Aging*, *29*(12), 1923–1929.

Carlson, S. W., Branden, M., Voss, K., Sun, Q., Rankin, C. A., & Gamblin, T. C. (2007). A complex mechanism for inducer mediated tau polymerization. *Biochemistry*, *46*(30), 8838–8849.

Chambers, C. B., Lee, J. M., Troncoso, J. C., Reich, S., & Muma, N. A. (1999). Overexpression of four-repeat tau mRNA isoforms in progressive supranuclear palsy but not in Alzheimer's disease. *Annals of Neurology*, *46*(3), 325–332.

Combs, B., & Gamblin, T. C. (2012). FTDP-17 tau mutations induce distinct effects on aggregation and microtubule interactions. *Biochemistry*, *51*(43), 8597–8607.

Combs, B., Voss, K., & Gamblin, T. C. (2011). Pseudohyperphosphorylation has differential effects on polymerization and function of tau isoforms. *Biochemistry*, *50*(44), 9446–9456.

Conrad, C., Zhu, J., Conrad, C., Schoenfeld, D., Fang, Z., Ingelsson, M., et al. (2007). Single molecule profiling of tau gene expression in Alzheimer's disease. *Journal of Neurochemistry*, *103*(3), 1228–1236.

Dinkel, P. D., Siddiqua, A., Huynh, H., Shah, M., & Margittai, M. (2011). Variations in filament conformation dictate seeding barrier between three- and four-repeat tau. *Biochemistry*, *50*(20), 4330–4336.

Gamblin, T. C., King, M. E., Kuret, J., Berry, R. W., & Binder, L. I. (2000). Oxidative regulation of fatty acid-induced tau polymerization. *Biochemistry*, *39*(46), 14203–14210.

Ghanem, D., Tran, H., Dhaenens, C. M., Schraen-Maschke, S., Sablonniere, B., Buee, L., et al. (2009). Altered splicing of Tau in DM1 is different from the foetal splicing process. *FEBS Letters*, *583*(4), 675–679.

Goedert, M., & Jakes, R. (1990). Expression of separate isoforms of human tau protein: Correlation with the tau pattern in brain and effects on tubulin polymerization. *The EMBO Journal*, *9*(13), 4225–4230.

Goedert, M., Spillantini, M. G., Crowther, R. A., Chen, S. G., Parchi, P., Tabaton, M., et al. (1999). Tau gene mutation in familial progressive subcortical gliosis. *Nature Medicine*, *5*(4), 454–457.

Goedert, M., Spillantini, M. G., Jakes, R., Rutherford, D., & Crowther, R. A. (1989). Multiple isoforms of human microtubule-associated protein tau: Sequences and localization in neurofibrillary tangles of Alzheimer's disease. *Neuron*, *3*(4), 519–526.

Goedert, M., Wischik, C. M., Crowther, R. A., Walker, J. E., & Klug, A. (1988). Cloning and sequencing of the cDNA encoding a core protein of the paired helical filament of Alzheimer disease: Identification as the microtubule-associated protein tau. *Proceedings of the National Academy of Sciences of the United States of America*, *85*(11), 4051–4055.

Goode, B. L., & Feinstein, S. C. (1994). Identification of a novel microtubule binding and assembly domain in the developmentally regulated inter-repeat region of tau. *The Journal of Cell Biology*, *124*(5), 769–782.

Gray, E. G., Paula-Barbosa, M., & Roher, A. (1987). Alzheimer's disease: Paired helical filaments and cytomembranes. *Neuropathology and Applied Neurobiology*, *13*(2), 91–110.

Grundke-Iqbal, I., Iqbal, K., Quinlan, M., Tung, Y. C., Zaidi, M. S., & Wisniewski, H. M. (1986). Microtubule-associated protein tau. A component of Alzheimer paired helical filaments. *The Journal of Biological Chemistry*, *261*(13), 6084–6089.

Himmler, A., Drechsel, D., Kirschner, M. W., & Martin, D. W., Jr. (1989). Tau consists of a set of proteins with repeated C-terminal microtubule-binding domains and variable N-terminal domains. *Molecular and Cellular Biology*, *9*(4), 1381–1388.

Hong, M., Zhukareva, V., Vogelsberg-Ragaglia, V., Wszolek, Z., Reed, L., Miller, B. I., et al. (1998). Mutation-specific functional impairments in distinct tau isoforms of hereditary FTDP-17. *Science*, *282*(5395), 1914–1917.

Horowitz, P. M., LaPointe, N., Guillozet-Bongaarts, A. L., Berry, R. W., & Binder, L. I. (2006). N-terminal fragments of tau inhibit full-length tau polymerization in vitro. *Biochemistry*, *45*(42), 12859–12866.

Houlden, H., Baker, M., Morris, H. R., MacDonald, N., Pickering-Brown, S., Adamson, J., et al. (2001). Corticobasal degeneration and progressive supranuclear palsy share a common tau haplotype. *Neurology*, *56*(12), 1702–1706.

Hutton, M., Lendon, C. L., Rizzu, P., Baker, M., Froelich, S., Houlden, H., et al. (1998). Association of missense and 5'-splice-site mutations in tau with the inherited dementia FTDP-17. *Nature*, *393*(6686), 702–705.

King, M. E., Ahuja, V., Binder, L. I., & Kuret, J. (1999). Ligand-dependent tau filament formation: Implications for Alzheimer's disease progression. *Biochemistry*, *38*(45), 14851–14859.

King, M. E., Gamblin, T. C., Kuret, J., & Binder, L. I. (2000). Differential assembly of human tau isoforms in the presence of arachidonic acid. *Journal of Neurochemistry*, *74*(4), 1749–1757.

Kosik, K. S., Orecchio, L. D., Bakalis, S., & Neve, R. L. (1989). Developmentally regulated expression of specific tau sequences. *Neuron*, *2*(4), 1389–1397.

Lacovich, V., Espindola, S. L., Alloatti, M., Pozo Devoto, V., Cromberg, L., Carna, M., et al. (2017). Tau isoforms imbalance impairs the axonal transport of the amyloid precursor protein in human neurons. *Journal of Neuroscience*, *37*(1), 58–69.

Lagunes, T., Herrera-Rivero, M., Hernandez-Aguilar, M. E., & Aranda-Abreu, G. E. (2014). Abeta(1-42) induces abnormal alternative splicing of tau exons 2/3 in NGF-induced PC12 cells. *Anais da Academia Brasileira de Ciências*, *86*(4), 1927–1934.

Lee, G., Neve, R. L., & Kosik, K. S. (1989). The microtubule binding domain of tau protein. *Neuron*, *2*(6), 1615–1624.

Levy, S. F., Leboeuf, A. C., Massie, M. R., Jordan, M. A., Wilson, L., & Feinstein, S. C. (2005). Three- and four-repeat tau regulate the dynamic instability of two distinct microtubule subpopulations in qualitatively different manners. Implications for neurodegeneration. *The Journal of Biological Chemistry*, *280*(14), 13520–13528.

Lippa, C. F., Zhukareva, V., Kawarai, T., Uryu, K., Shafiq, M., Nee, L. E., et al. (2000). Frontotemporal dementia with novel tau pathology and a Glu342Val tau mutation. *Annals of Neurology*, *48*(6), 850–858.

Mattson, M. P., Mark, R. J., Furukawa, K., & Bruce, A. J. (1997). Disruption of brain cell ion homeostasis in Alzheimer's disease by oxy radicals, and signaling pathways that protect therefrom. *Chemical Research in Toxicology*, *10*(5), 507–517.

Novak, M., Jakes, R., Edwards, P. C., Milstein, C., & Wischik, C. M. (1991). Difference between the tau protein of Alzheimer paired helical filament core and normal tau revealed by epitope analysis of monoclonal antibodies 423 and 7.51. *Proceedings of the National Academy of Sciences of the United States of America*, *88*(13), 5837–5841.

Ong, W. Y., Farooqui, T., & Farooqui, A. A. (2010). Involvement of cytosolic phospholipase A(2), calcium independent phospholipase A(2) and plasmalogen selective phospholipase A(2) in neurodegenerative and neuropsychiatric conditions. *Current Medicinal Chemistry*, *17*(25), 2746–2763.

Panda, D., Samuel, J. C., Massie, M., Feinstein, S. C., & Wilson, L. (2003). Differential regulation of microtubule dynamics by three- and four-repeat tau: Implications for the onset of neurodegenerative disease. *Proceedings of the National Academy of Sciences of the United States of America*, *100*(16), 9548–9553.

Paranjape, S. R., Riley, A. P., Somoza, A. D., Oakley, C. E., Wang, C. C., Prisinzano, T. E., et al. (2015). Azaphilones inhibit tau aggregation and dissolve tau aggregates in vitro. *ACS Chemical Neuroscience*, *6*(5), 751–760.

Poorkaj, P., Muma, N. A., Zhukareva, V., Cochran, E. J., Shannon, K. M., Hurtig, H., et al. (2002). An R5L tau mutation in a subject with a progressive supranuclear palsy phenotype. *Annals of Neurology*, *52*(4), 511–516.

Rankin, C. A., Sun, Q., & Gamblin, T. C. (2005). Pseudo-phosphorylation of tau at Ser202 and Thr205 affects tau filament formation. *Brain Research. Molecular Brain Research*, *138*(1), 84–93.

Reynolds, M. R., Berry, R. W., & Binder, L. I. (2005). Site-specific nitration differentially influences tau assembly in vitro. *Biochemistry*, *44*(42), 13997–14009.

Rosso, S. M., van Herpen, E., Deelen, W., Kamphorst, W., Severijnen, L. A., Willemsen, R., et al. (2002). A novel tau mutation, S320F, causes a tauopathy with inclusions similar to those in Pick's disease. *Annals of Neurology*, *51*(3), 373–376.

Schoch, K. M., DeVos, S. L., Miller, R. L., Chun, S. J., Norrbom, M., Wozniak, D. F., et al. (2016). Increased 4R-tau induces pathological changes in a human-tau mouse model. *Neuron*, *90*(5), 941–947.

Sergeant, N., Delacourte, A., & Buee, L. (2005). Tau protein as a differential biomarker of tauopathies. *Biochimica et Biophysica Acta*, *1739*(2–3), 179–197.

Sharon, R., Bar-Joseph, I., Mirick, G. E., Serhan, C. N., & Selkoe, D. J. (2003). Altered fatty acid composition of dopaminergic neurons expressing alpha-synuclein and human brains with alpha-synucleinopathies. *The Journal of Biological Chemistry*, *278*(50), 49874–49881.

Snowden, S. G., Ebshiana, A. A., Hye, A., An, Y., Pletnikova, O., O'Brien, R., et al. (2017). Association between fatty acid metabolism in the brain and Alzheimer disease neuropathology and cognitive performance: A nontargeted metabolomic study. *PLoS Medicine, 14*(3), e1002266.

Trabzuni, D., Wray, S., Vandrovcova, J., Ramasamy, A., Walker, R., Smith, C., et al. (2012). MAPT expression and splicing is differentially regulated by brain region: Relation to genotype and implication for tauopathies. *Human Molecular Genetics*, *21*(18), 4094–4103.

von Bergen, M., Barghorn, S., Muller, S. A., Pickhardt, M., Biernat, J., Mandelkow, E. M., et al. (2006). The core of tau-paired helical filaments studied by scanning transmission electron microscopy and limited proteolysis. *Biochemistry*, *45*(20), 6446–6457.

Voss, K., & Gamblin, T. C. (2009). GSK-3β phosphorylation of functionally distinct tau isoforms has differential, but mild effects. *Molecular Neurodegeneration*, *4*(18), 1–12.

Wegmann, S., Medalsy, I. D., Mandelkow, E., & Muller, D. J. (2013). The fuzzy coat of pathological human Tau fibrils is a two-layered polyelectrolyte brush. *Proceedings of the National Academy of Sciences of the United States of America*, *110*(4), E313–E321.

Wischik, C. M., Novak, M., Thogersen, H. C., Edwards, P. C., Runswick, M. J., Jakes, R., et al. (1988). Isolation of a fragment of tau derived from the core of the paired helical filament of Alzheimer disease. *Proceedings of the National Academy of Sciences of the United States of America*, *85*(12), 4506–4510.

Wood, J. G., Mirra, S. S., Pollock, N. J., & Binder, L. I. (1986). Neurofibrillary tangles of Alzheimer disease share antigenic determinants with the axonal microtubule-associated protein tau (tau). *Proceedings of the National Academy of Sciences of the United States of America*, *83*(11), 4040–4043.

Yoshida, M. (2006). Cellular tau pathology and immunohistochemical study of tau isoforms in sporadic tauopathies. *Neuropathology*, *26*(5), 457–470.